

Angular distributions of scattered excited muonic hydrogen atoms

V. N. Pomerantsev, V. P. Popov

Institute of Nuclear Physics, Moscow State University, 119899 Moscow, Russia

Submitted 10 January 2006

Resubmitted 6 March 2006

Coulomb deexcitation differential cross sections of excited muonic hydrogen in collisions with hydrogen atom are studied for the first time. In the fully quantum-mechanical close-coupling approach both the differential cross sections for the $nl \rightarrow n'l'$ transitions and l -averaged differential cross sections have been calculated for the initial exotic atom states with $n = 2 - 6$ at kinetic energies $E_{\text{cm}} = 0.01 - 15$ eV and for scattering angles $\theta_{\text{cm}} = 0 - 180^\circ$. The vacuum polarization shifts of the ns -states are taken into account. The differential cross sections of the elastic and Stark scattering obtained in the same approach are also presented. The main features of the calculated differential cross sections are discussed and a strong anisotropy of Coulomb deexcitation cross sections is predicted.

PACS: 36.10.-k

Introduction. Exotic hydrogen-like atoms are formed in excited states, when heavy negative particles (μ^- , π^- , etc.) are slowed down and captured in hydrogen media. The following atomic cascade of collisional and radiative transitions proceeds via many intermediate states up to nuclear absorption or transition to the ground state occurs. Since the experimental data are mainly available for the last stage of this atomic cascade, the reliable knowledge of the total and differential cross sections (DCS) of the collisional processes is needed for the realistic analysis of these data. In particular, the processes

$$(\mu^- p)_{nl} + H_{1s} \rightarrow (\mu^- p)_{n'l'} + H_{1s} \quad (1)$$

of the elastic scattering ($n' = n$, $l' = l$), Stark transitions ($n' = n$, $l' \neq l$), and Coulomb deexcitation ($n' < n$) essentially change the energy- and nl -distributions of exotic atoms. It is especially important from the view of the precise experiments at Paul Scherrer Institut with muonic [1] and pionic [3] hydrogen atoms. These experiments are aimed at the extraction of the root mean squared proton charge radius with the relative accuracy of 10^{-3} from the Lamb shift experiment [1] and the determination of the πN scattering lengths with the accuracy better than 1% by extracting the strong interaction shift and width of the pionic hydrogen $1s$ -state [3]. The proper analysis of these experiments requires a reliable theoretical treatment of related cascade processes.

The Coulomb deexcitation (CD) plays an important role in the kinetic energy distribution of the exotic atoms. In particular, the kinetic energy distribution of $(\mu^- p)$ - and $(\pi^- p)$ -atoms during the radiative transitions $np \rightarrow 1s$ have significant high-energy components

resulting from the preceding CD transitions. Before the recent paper [3] the only $\Delta n = 1$ transitions are assumed to be important in the Coulomb transitions at low n . Moreover, it is also suggested in the cascade calculations [4] that the CD process results in the isotropic angular distribution.

The first study of the elastic and Stark scattering DCS in the exotic atom - hydrogen atom collisions has been performed within the quantum-mechanical adiabatic approach [5]. Later, the cross sections were also calculated in the framework of the close-coupling model and semiclassical approximation [6] where the Coulomb interaction of the exotic atom with the hydrogen atom field is modeled by the screening dipole approximation. This approximation becomes invalid at low collisional energies below some value E^* , which depends on the principal quantum number n (see [7]). Thus, the latter approach as well as various modifications of the semiclassical model [8, 9] can result in uncontrolled errors in the low-energy region where only a few partial waves are important.

The main goal of this paper is to introduce the first theoretical study of the Coulomb deexcitation differential cross sections in the muonic atom - hydrogen atom collisions. In particular, we are interested in the main features of the n and E dependences of these cross sections. Our new results, concerning the DCS of elastic and Stark scattering are also presented.

In the present paper the DCS of the processes (1) are studied in the framework of the more accurate close-coupling (CC) approach. The approach has been developed earlier [10] by the authors to describe the elastic scattering and Stark transitions in the exotic atom -

hydrogen molecule collisions and has been employed recently [3] for unified treatment of the processes (1). In the CC approach the first fully quantum-mechanical calculations of the total CD cross sections both for muonic [3] and pionic [11] hydrogen atoms have been performed. The calculations of the total CD cross sections have been also performed earlier within a number of other approaches [6, 12–15]. While the semiclassical model [12] and classical-trajectory model [6] cannot be suitable for treating the low n states, the more elaborated calculations within the advanced adiabatic approximation [13–15] give much smaller values for cross sections than ones obtained in [12] and in our recent CC calculations [3].

Approach. In the framework of the CC approach the total wave function of the four-body system is expanded in terms of the basis states with the conserving quantum numbers of the total angular momentum JM and parity $\pi = (-1)^{l+L}$. The basis states are chosen as tensor products of the free exotic and hydrogen atom wave functions and the angular wave function of their relative motion. The basis includes all states of the exotic atom corresponding to the open channels. The expansion results in the set of the coupled differential equations. In contrast with [6], the interaction potential matrix for the exact four-body Coulomb interaction of the colliding atoms is calculated analytically in the present approach. Moreover, as it is shown in [3] the approximation similar to “dipole approximation” results in an improper description of the CD process.

At fixed E_{cm} (energy of collision in the center of mass system) and given J and π the set of the coupled equations are solved numerically by the Numerov method with the standing-wave boundary conditions involving the K -matrix. The corresponding T -matrix is obtained from the K matrix using the matrix equation $T = 2iK(I - iK)^{-1}$. In the present study, as distinct from paper [3], we take into account the vacuum polarization energy shifts of the ns states which are especially important for lower exotic atom states and kinetic energies comparable with the energy shift value¹⁾.

The formalism has been described in more details in [3]. Here we give the formulae for the DCS discussed below. The DCS for the transition from the initial state (nl) to the final state ($n'l'$) are defined as

$$\frac{d\sigma_{nl \rightarrow n'l'}}{d\Omega} = \frac{1}{2l+1} \frac{k_f}{k_i} \sum_{mm'} |f_{nlm \rightarrow n'l'm'}(k_i, k_f; \Omega)|^2, \quad (2)$$

¹⁾The $2s - 2p$ energy splitting $\Delta\epsilon_{2s-2p}$ for the muonic hydrogen atom is equal to 0.206 eV and this splitting decreases approximately as n^{-3} with n increasing.

where the scattering amplitude is given by

$$f_{nlm \rightarrow n'l'm'}(k_i, k_f; \Omega) = \frac{2\pi i}{\sqrt{k_i k_f}} \sum_{JLL'\lambda'} i^{L'-L} Y_{L0}^*(0) \times \\ \times \langle lmL0 | Jm \rangle T_{nlL \rightarrow n'l'L'}^J \langle l'm'L'\lambda' | Jm \rangle Y_{L'\lambda'}(\Omega). \quad (3)$$

Here, k_i and k_f are the initial and final relative momenta, correspondingly; $\Omega \equiv \theta, \varphi$, where θ is the cms scattering angle, and $T_{i \rightarrow f}^J$ is the transition matrix. The indices of the entrance channel and the target electron state are omitted for brevity.

In order to illustrate the most general features of DCS, we introduce the cross sections averaged over the initial angular momentum l of the exotic atom. The following l -averaged angular distributions are defined

$$\frac{d\sigma_n^{el}}{d\Omega} = \frac{1}{n^2} \sum_l (2l+1) \frac{d\sigma_{nl \rightarrow nl}}{d\Omega}, \\ \frac{d\sigma_n^{St}}{d\Omega} = \frac{1}{n^2} \sum_{l,l'} (1 - \delta_{ll'}) (2l+1) \frac{d\sigma_{nl \rightarrow n'l'}}{d\Omega}, \quad (4) \\ \frac{d\sigma_{n \rightarrow n'}^{CD}}{d\Omega} = \frac{1}{n^2} \sum_{l,l'} (2l+1) \frac{d\sigma_{nl \rightarrow n'l'}}{d\Omega}, \quad n' < n,$$

for the elastic scattering, Stark transitions and CD processes. Hereafter, the atomic units will be used throughout the paper and the collision energy will be referred to the states with $l \neq 0$ in the entrance channel, which are assumed to be degenerated.

Results. The numerical calculations of the DCS for the collisional processes (1) have been done for $(\mu p)_n$ atoms with the initial values $n = 2 - 6$ at energies $E_{cm} = 0.01 - 15$ eV and at all the scattering angles θ_{cm} from zero up to 180° . Some of our results are presented in Figs.1–6.

In Figs.1a and 1b the DCS for $2p \rightarrow 2p, 2s$ (elastic and Stark scattering) and $2p \rightarrow 1s$ (CD) transitions at $E_{cm} = 0.01$ eV and 1 eV (referring to the $2p$ threshold) are shown. It is worthwhile noting that the relative motion energy in the entrance channel for the $2s \rightarrow 2s, 2p$ and $2s \rightarrow 1s$ transitions increases on the 0.206 eV due to the Lamb shift in comparison with the scattering processes in the $2p$ state. As it is seen from Fig.1a, the angular distributions of the elastic $2p \rightarrow 2p$ scattering and Coulomb $2p \rightarrow 1s$ transition are similar and almost isotropic due to contributions of the S -wave relative motion with a small mixture of the P -wave. It is also seen that CD process for $2p \rightarrow 1s$ transition is more than four order of the magnitude suppressed relatively to the $2p \rightarrow 2p$ elastic scattering and more or about two order of the magnitude as compared with both the Stark

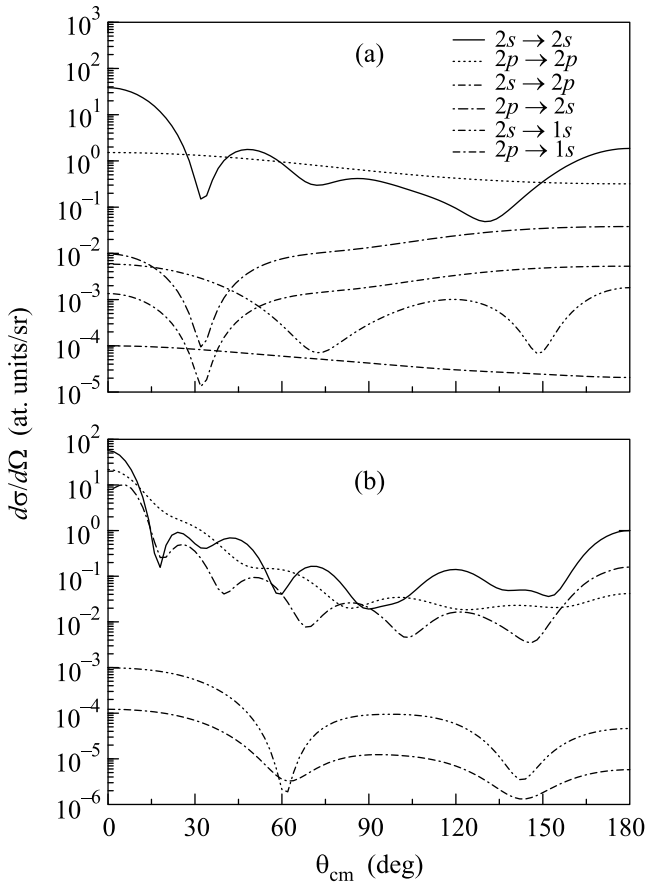


Fig.1. Differential cross sections for $2l \rightarrow 2l'$ and $2l \rightarrow 1s$ transitions in $(\mu p)_{2l} + H$ collisions vs. cms scattering angle θ_{cm} at $E_{cm} = 0.01$ eV (a) and 1 eV (b) (referring to $2p$ state)

$2p \rightarrow 2s$ and Coulomb $2s \rightarrow 1s$ DCS, respectively. The Stark transitions $2p \rightarrow 2s$ and $2s \rightarrow 2p$ are inelastic and that results in their quite unusual angular distributions (see Fig. 1a) with the maximum at zero scattering angle and minimum at $\theta_{cm} \sim 30^\circ$ and smooth increasing at the backward hemisphere.

In the DCS of the elastic $2s \rightarrow 2s$ scattering ($E_{cm} = 0.216$ eV) we see the structures (due to higher partial waves, involved in the scattering process) as compared with the almost isotropic DCS for $2p \rightarrow 2p$ transition. The comparison of the DCS of the Stark transitions, presented in Figs. 1a and 1b, shows a significant effect of the Lamb shift on these cross sections, which changes substantially depending on the ratio value of the $E_{cm}/\Delta\varepsilon_{2s-2p}$. The Stark DCS of the $2p \rightarrow 2s$ and $2s \rightarrow 2p$ transitions at low kinetic energy comparable with the Lamb shift value have quite different behavior in comparison with the elastic ones and reveal a strong suppression in the forward hemisphere by more than three order of the magnitude. When the energy of the collision is much larger than $\Delta\varepsilon_{2s-2p}$ we observe the usual

picture [5, 6] of the DCS for Stark transitions with a strong forward peak and a set of maxima and minima (see Fig.1b).

CD process occurs at essentially smaller distances than the elastic and Stark processes and the number of partial waves involved in the CD process, as a rule, is much smaller. A strong centrifugal barrier prevents the colliding atoms from penetrating in the interaction region. Besides, at smaller value n the number of the partial waves contributing to the CD process (at the fixed energy) also decreases.

In particular, the DCS of the CD process in case of $n = 2$ have a quite simple angular dependence due to a few partial waves involved in the process (see Fig.1). The angular dependences of the DCS for $2s \rightarrow 1s$ and $2p \rightarrow 1s$ Coulomb transitions are mainly determined by the contributions of the lowest partial waves of the relative motion at all energies under consideration. The DCS of these Coulomb transitions as it is seen in Fig.1b have a similar angular dependence which shape is slowly changed enhancing the forward hemisphere scattering with energy increasing.

It is well-known that in the muonic hydrogen atoms, the $2s$ -state plays a particular role due to $2s$ Lamb shift and has no analog in the other exotic atoms in which the strong interaction leads to a large rate of the nuclear absorption from this state. In particular, a new knowledge about the collisional quenching of $2s$ state at collisional energy near or below $2p$ threshold is of special interest. As it shown in Fig.1a, the DCS for the $2p \rightarrow 1s$ transition is strongly suppressed about two order of the magnitude compared with the $2s \rightarrow 1s$ transition and this suppression is also observed at higher energy (see Fig.1b). Hence the $2s \rightarrow 1s$ transition determines the CD $2 \rightarrow 1$ transition at all kinetic energies and it is quite probable that the observed collisional quenching of the metastable $2s$ state and the high energy component of the muonic hydrogen in $1s$ state can be explained by the direct CD process.

The typical angular distributions for the individual $nl \rightarrow n'l'$ transitions for $n = 5$ are shown in Fig.2a and 2b for the elastic and Stark scattering, respectively. It is well known [5, 6] that DCS of these processes are similar to the diffraction scattering (at the collisional energies more or about 1 eV) with a strong forward peak which is enhanced with increasing energy. While the elastic cross sections always have a strong peak at $\theta_{cm} = 0$, the first maximum position in the Stark DCS depends on the $\Delta l = |l - l'|$ value. In particular, for $\Delta l = 1$ this maximum is at finite scattering angles as it is also remarked in [6]. According to our calculations, the sharpest variations in DCS are always observed in

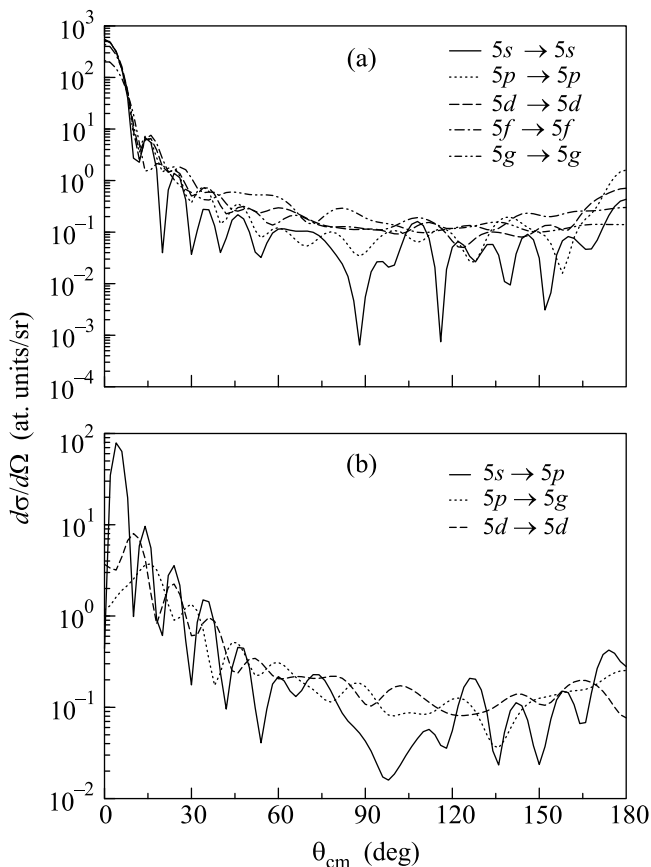


Fig.2. Differential elastic (a) and Stark (b) cross sections for $(\mu p)_{sl} + H$ collisions vs. cms scattering angle θ_{cm} at $E_{cm} = 1$ eV.

the $ns \rightarrow n's$ and $ns \rightarrow n'p$ transitions (see also Fig.5 for DCS of the CD process). The forward hemisphere first and next peaks in elastic scattering (see Fig.2a) and Stark transitions (see Fig.2b) have a tendency to be less pronounced and the corresponding angular distribution becomes smoother with the increase of l and Δl . In contrast, the forward hemisphere peak is sharper with n increasing.

The energy dependence of the l -averaged DCS for the elastic scattering is illustrated in Fig.3 for $n = 4$. While the DCS for the individual elastic $nl \rightarrow nl$ transitions (the same is valid for the Stark $nl \rightarrow nl'$ transitions) reveal the complicated structure, the l -averaged cross sections smooth out many details and allow to study the most general features of the process. It is seen, that at low energies ($\lesssim 1$ eV) the DCS can be approximated by a constant for the simple estimation at θ_{cm} more or about 75° . However, at higher energies the appreciable enhancing of the backward scattering is observed.

The l -averaged Stark DCS at $E_{cm} = 1$ eV for different values of n are shown in Fig.4. One can see that

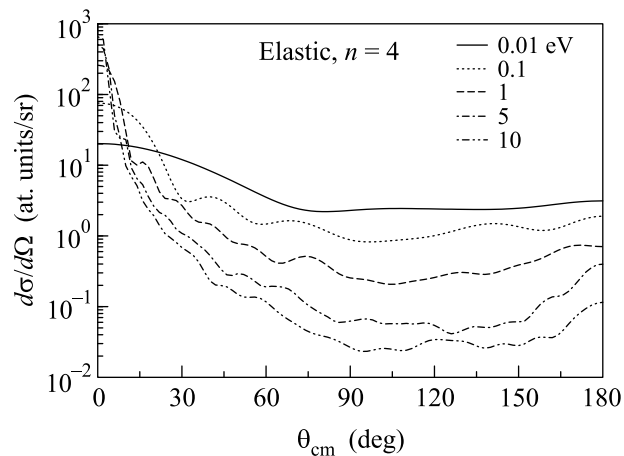


Fig.3. The l -average differential elastic cross sections for $(\mu p)_{n=4} + H$ collisions at different energies

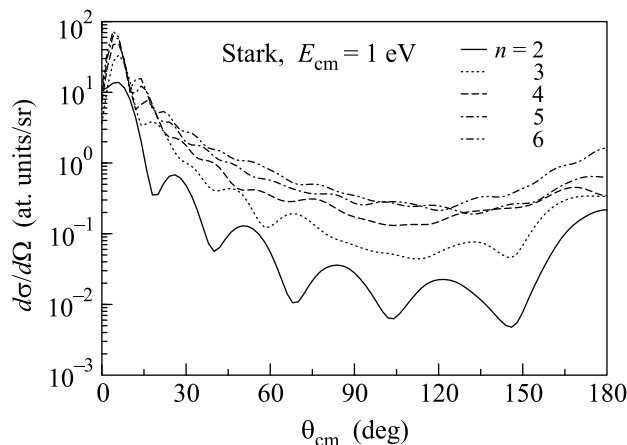


Fig.4. The l -average differential Stark cross sections for $(\mu p)_n + H$ collisions ($n = 2 - 6$) at $E_{cm} = 1$ eV

with the increase of n the first forward peak also becomes sharper and narrower (as well as for the elastic scattering) but remains to be at the finite values of scattering angle. The height of this peak depends on n not so strong as the diffraction maximum in elastic scattering (cf. Figs.3 and 4). The diffraction structure of minima and maxima becomes less pronounced with increasing n . As a whole our results for the elastic and Stark DCS are in a qualitative agreement with the previous calculations [5, 6].

Now we are coming to the discussion of the typical angular distributions for the CD process. The calculations of these DCS have not been reported until now and in the cascade calculations the angular distributions of the CD process are presumed to be isotropic. The calculated DCS for individual $nl \rightarrow n'l'$ transitions with $\Delta n = 1$ and 2 at $E_{cm} = 1$ eV are shown in Figs.5a and 5b, respectively. In Fig.6 the l -averaged DCS for the

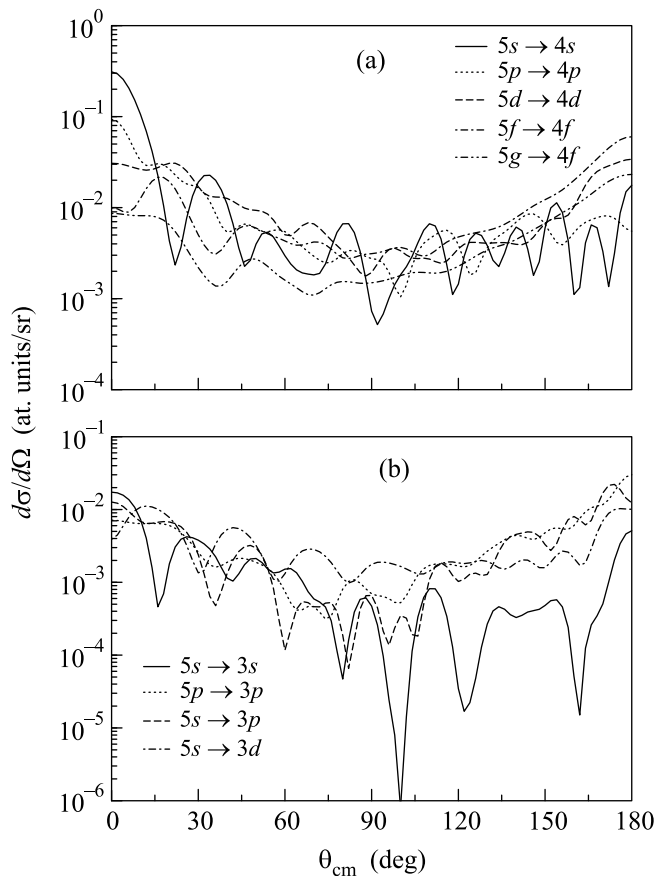


Fig.5. Differential CD cross sections for the individual transitions with $\Delta n = 1$ (a) and $\Delta n = 2$ (b) for $(\mu p)_{n=5} + H$ collisions at $E_{cm} = 1$ eV

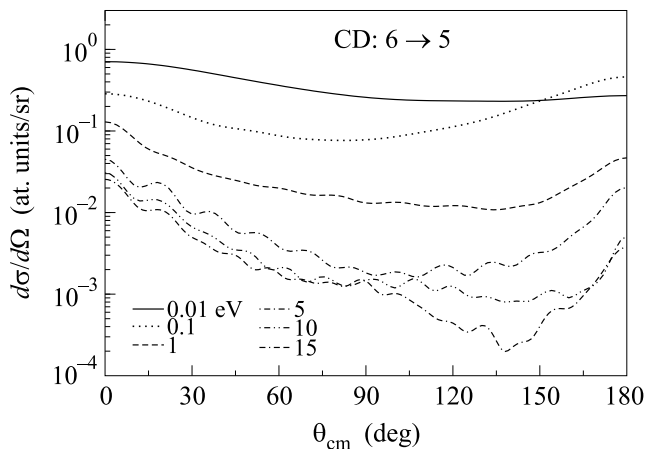


Fig.6. The l -average CD differential cross sections for the $6 \rightarrow 5$ transition in $(\mu p)_{n=6} + H$ collisions at different energies

$6 \rightarrow 5$ transition at different energy from 0.01 up to 15 eV are presented. Our study reveals the following main features of the CD angular distributions.

The angular distributions both of the individual and l -averaged cross sections (excluding very low energies) are far from isotropic: as a whole the scattering at $\theta_{cm} \lesssim 60^\circ$ and $\theta_{cm} > 120^\circ$ is noticeably enhanced. The DCS for $ns \rightarrow n's$ transitions (see Figs.5) have (as for elastic scattering) a more pronounced diffraction structure with sharp maxima and minima and a strong peak at zero angle as compared with the smoother angular dependence for other CD transitions. This behaviour can be simply explained by the conditions $L = L' = J$ (for $ns \rightarrow n's$ transitions) which strongly reduce the number of terms in the amplitude (3) in contrast with the other transitions. The increase of kinetic energy enhances asymmetry in the angular dependence of the l -averaged DCS and decreases the role of the backward scattering (see Fig.6).

Summary. The fully quantum-mechanical CC approach has been applied for the calculations of the elastic scattering, Stark transition and Coulomb deexcitation DCS in a self-consistent manner and the detailed analysis of the obtained results has been performed. For the first time the DCS of the CD process have been calculated for the values of the principal quantum number and kinetic energy relevant for kinetics of the atomic cascade. The first results for the direct collisional quenching of the $2s$ -state due to CD process were also obtained. The present study reveals the new knowledge about the CD process and is very important for the reliable analysis of the K X -ray yields and high energy component in the kinetic energy distribution of muonic hydrogen atoms. We hope that our study allows to remove some uncertainties inherent in the previous cascade calculations, which resulted from the treatment of collisions, especially Coulomb deexcitation, involving different and not always self-consistent approximations.

We are grateful to Prof. L.I. Ponomarev for permanent interest in our studies and support. This work was supported by Russian Foundation for Basic Research.

1. F. Kottmann, W. Amir, F. Biraben et al., *Hyperfine Interact.* **138**, 55 (2001).
2. D. Gotta, *πN Newsletter* **15**, 276 (1999).
3. G. Ya. Korenman, V. N. Pomerantsev, and V. P. Popov, *JETP Lett.* **81**, 543 (2005); nucl-th/0501036.
4. T. S. Jensen and V. E. Markushin, *Eur. Phys. Journ. D* **21**, 271 (2002).
5. V. P. Popov and V. N. Pomerantsev, *Hyperfine Interact.* **119**, 137 (1999).
6. T. S. Jensen and V. E. Markushin, *PSI-PR-99-32*(1999); *Eur. Phys. Journ. D* **19**, 165 (2002); *D* **21**, 261 (2002).
7. V. V. Gusev, V. P. Popov, and V. N. Pomerantsev, *Hyperfine Interact.* **119**, 141 (1999).

8. V. Bystritsky, W. Czaplinski, J. Wozniak et al., Phys. Rev. A **53**, 4169 (1996).
9. T. P. Terada and R. S. Hayano, Phys. Rev. C **55**, 73 (1997).
10. V. P. Popov and V. N. Pomerantsev, Hyperfine Interact. **138**, 109 (2001).
11. V. N. Pomerantsev and V. P. Popov, nucl-th/0511026.
12. L. Bracci and G. Fiorentini, Nuovo Cim. A **43**, 9 (1978).
13. L. I. Ponomarev and E. A. Solov'ev, JETP Lett. **64**, 135 (1996).
14. A. V. Kravtsov, A. I. Mikhailov, L. I. Ponomarev, and E. A. Solovyev, Hyperfine Interact. **138**, 99 (2001).
15. L. I. Ponomarev and E. A. Solovyov, Yad. Fiz. **65**, 1615 (2002).